

AD-A104 020

PLASMA JOINING OF METAL MATRIX COMPOSITES(U) MSNM INC  
SAN MARCOS CA G H RAYNOLDS ET AL. JUN 87  
ARO-22817. 6-MS-S DAG29-85-C-0027

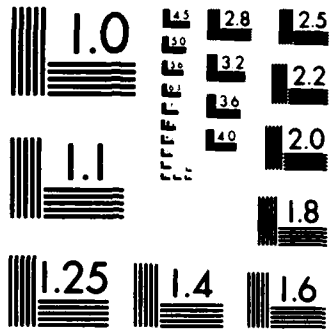
1/1

UNCLASSIFIED

F/G 11/4

NL





MICROCOPY RESOLUTION TEST CHART  
NATIONAL BUREAU OF STANDARDS 1963 A

ARC 22817.6-1955

(2)

**MSNW, INC.**

P.O. Box 865  
San Marcos, California 92069  
(619) 744-7648

AD-A184 828

**PLASMA JOINING OF METAL MATRIX COMPOSITES**

Submitted to U.S. Army Research Office

Contract No. DAAG29-85-C-0027

Interim Technical Report - October 1986 - January 1987

Prepared by:  
G.M. Reynolds and L. Yang, MSNW, Inc.

**DTIC**  
**ELECTE**  
SEP 17 1987  
**S** **D**  
CKE

This document has been prepared  
for public release and sale,  
distribution is unlimited.

UNCLASSIFIED

SECURITY CLASSIFICATION OF THIS PAGE (When Data Entered)

REPORT DOCUMENTATION PAGE		READ INSTRUCTIONS BEFORE COMPLETING FORM	
1. REPORT NUMBER <b>ARO 22817.6-MS-5</b>	2. GOVT ACCESSION NO. <b>ADA184828</b>	3. RECIPIENT'S CATALOG NUMBER N/A	
4. TITLE (and Subtitle)  Plasma Joining of Metal Matrix Composites		5. TYPE OF REPORT & PERIOD COVERED Interim Technical October 1986-January 1987	
		6. PERFORMING ORG. REPORT NUMBER N.A.	
7. AUTHOR(s)  G.H. Reynolds and L. Yang		8. CONTRACT OR GRANT NUMBER(s)  DAAG29-85-C-0027	
9. PERFORMING ORGANIZATION NAME AND ADDRESS MSNW, Inc. P.O. Box 865 San Marcos, CA 92069		10. PROGRAM ELEMENT, PROJECT, TASK AREA & WORK UNIT NUMBERS	
11. CONTROLLING OFFICE NAME AND ADDRESS U. S. Army Research Office Post Office Box 12211 Research Triangle Park, NC 27709		12. REPORT DATE June 1987	
14. MONITORING AGENCY NAME & ADDRESS (if different from Controlling Office)		13. NUMBER OF PAGES 10	
		15. SECURITY CLASS. (of this report) Unclassified	
16. DISTRIBUTION STATEMENT (of this Report)  Approved for public release; distribution unlimited.		15a. DECLASSIFICATION/DOWNGRADING SCHEDULE	
17. DISTRIBUTION STATEMENT (of the abstract entered in Block 20, if different from Report)  NA			
18. SUPPLEMENTARY NOTES  The view, opinions, and/or findings contained in this report are those of the author(s) and should not be construed as an official Department of the Army position, policy, or decision, unless so designated by other documentation.			
19. KEY WORDS (Continue on reverse side if necessary and identify by block number)  Composite materials, joining, plasma processing, thermochemistry.			
20. ABSTRACT (Continue on reverse side if necessary and identify by block number)  Microstructural and microchemical changes occurring in the heat affected zone, at the fusion line, and in the weld metal of low pressure, transferred arc plasma process welds produced with composite powder filler metals are described.			

DD FORM 1 JAN 73 1473

EDITION OF 1 NOV 65 IS OBSOLETE

UNCLASSIFIED

SECURITY CLASSIFICATION OF THIS PAGE (When Data Entered)

ABSTRACT

Microstructural and microchemical changes occurring in the heat affected zone, at the fusion line, and in the weld metal of low pressure, transferred arc plasma process welds produced with composite powder filler metals are described.

EXPERIMENTAL RESULTS

Electron beam microprobe examinations were made on near-fusion line regions of butt welds produced in 6061-30 wt. % SiC<sub>p</sub> base plates using a low pressure, transferred arc plasma welding process which employed composite powder filler metals. Microstructural and microchemical changes occurring in plasma processed filler metal powders and in plasma deposited bulk material produced on inert substrates have been described in previous reports. The filler metal compositions, identical to those used previously, were 1100 aluminum - 30 wt. % SiC<sub>p</sub>, aluminum - 3 wt. % Zr - 30 wt. % SiC<sub>p</sub> and aluminum - 5 wt. % Ti - 30 wt. % SiC<sub>p</sub>.

Figure 1. shows a backscattered electron image of the near-fusion line microstructures observed for a weld produced using 1100 aluminum - 30 wt. % SiC<sub>p</sub> filler metal and also shows the path of the electron beam microprobe trace across the fusion line. The most interesting feature of the micrograph is the band of light colored material along the fusion line. In optical metallographic examination, this band appeared to be free of SiC particulates, however electron metallographic examination revealed that this band actually contains very finely dispersed SiC fragments. These apparently form by

Availability Codes	
Dist	Avail and/or Special
A-1	



disintegration of the large SiC particulates present in the starting filler metal and present intact throughout most of the weld metal microstructure. Isolated islands of matrix phase containing very fine SiC particulates were also found in the weld metal microstructure.

Figure 2. shows a similar micrograph of a weld produced using aluminum - 3 wt. % Zr - 30 wt. % SiC<sub>p</sub> filler metal. The band of light colored material containing finely dispersed SiC along the fusion line is much narrower for this filler metal composition but still present. No islands of matrix phase containing finely divided SiC particulates were found in the weld metal microstructure.

Figure 3. shows a similar micrograph of a weld produced using aluminum - 5 wt. % Ti - 30 wt. % SiC<sub>p</sub> filler metal. No band of material containing finely dispersed SiC is present along the fusion line. No islands of matrix phase containing finely divided SiC particulates were found in the weld metal microstructure.

The 1100 aluminum - 30 wt. % SiC<sub>p</sub> filler metal composition would be expected to show the most extensive matrix/reinforcing phase chemical reactions during plasma processing. The tendency for formation of regions containing very finely dispersed SiC particulates at the fusion line and in the bulk of the weld metal may be related to the extent of such reactions during plasma processing. Disintegration of the large SiC particulates present in the starting filler material is obviously less in those filler metal compositions containing reactive metal additions. The reactive metal additions also reduce the likelihood of interfacial Al<sub>4</sub>C<sub>3</sub> formation by matrix/reinforcing chemical

interactions. The effect of the fusion line microstructural zone will receive particular attention in the evaluation of weldment mechanical properties.

Figure 4. shows electron beam microprobe traces for Si and C across the heat affected zone, fusion line and weld metal on the path shown in Figure 1. The path traverses two large SiC particles, A which is in the weld metal and B which is in the heat affected zone. The "band" refers to the fusion line microstructural zone containing finely divided SiC. The traces do not provide sufficient resolution for positive identification of interfacial reactions however they suggest the possibility of such reactions at the fusion line (in the "band") where the peak Si and C concentrations are not in synchronization as they should be for unreacted SiC.

Figure 5. shows similar microprobe traces for Si, C, and Zr across the heat affected zone, fusion line and weld metal on the path shown in Figure 2. The path traverses large SiC particles A in the weld metal and B in the heat affected zone. No evidence of possible interfacial reactions is noted at or near the fusion line. No evidence for Zr diffusion into the base metal is observed. The Zr concentration spikes in the weld metal are locations of the  $Al_3Zr$  second phase present in the matrix alloy.

Figure 6. shows similar microprobe traces for Si, C, and Ti across the heat affected zone, fusion line and weld metal on the path shown in Figure 3. The path traverses large SiC particles A in the weld metal and B, C and D in the heat affected zone. The fusion line interface is quite sharp with no band present. No evidence for particle/matrix interfacial chemical interaction is resolved in either the weld or heat affected zone. No evidence for Ti

diffusion into the base metal is observed.

Additional filler metal compositions having higher Ti and Zr concentrations are being synthesized for use in preparation of welds for mechanical property studies.



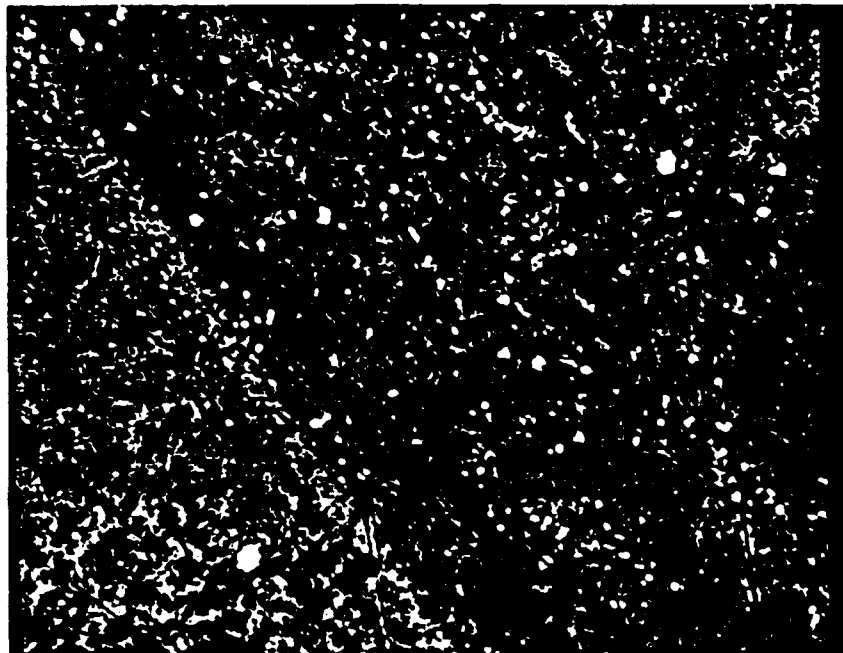


Figure 1. Fusion line and heat affected zone region of low pressure plasma deposited weld produced with 1100 aluminum - 30 wt. % SiC filler metal. Heat affected zone is at lower left, weld metal at upper right. Note band of lighter material which contains only very fine SiC particles along fusion line. Path of microprobe trace is shown. Backscattered electron image. Magnification 560X.

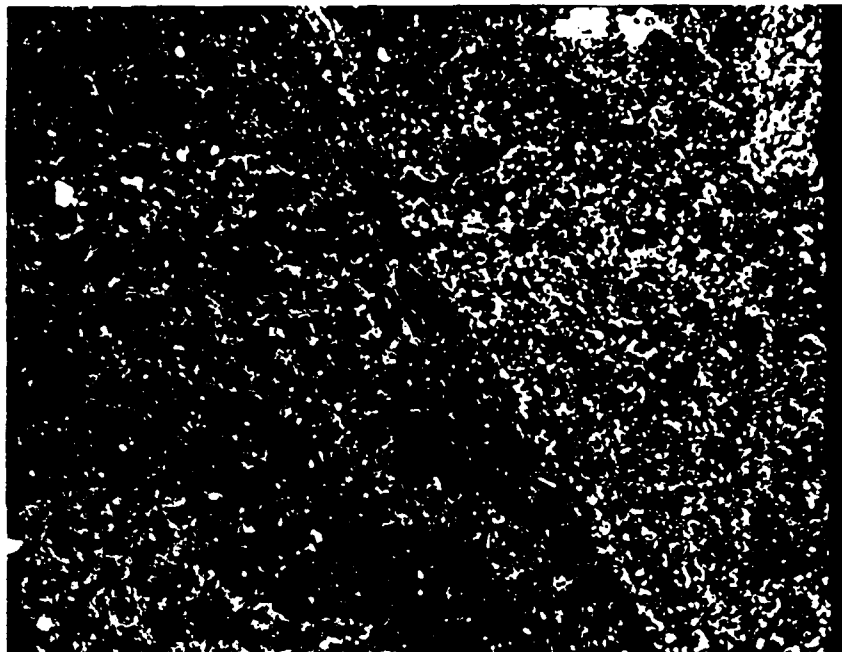


Figure 3. Fusion line and heat affected zone region of low pressure plasma deposited weld produced with aluminum - 5 wt. % Ti - 30 wt. % SiC<sub>2</sub> filler metal. Heat affected zone is to the left, weld metal to the right. Note absence of lighter material along fusion line. Path of microprobe trace is shown. Backscattered electron image. Magnification 400X.

CAMECA-MICROBEAM  
10-DEC-85  
STEP SCANNING

AUTO SCALE

Polar Angle = 0  
1100

SP1 : ODPB  
MAX = 1057

Lambda = 44.94 Angstrom  
C<sub>Kα</sub>

SP2 : TAP

MAX = 102769

Lambda = 7.13 Angstroms  
Si<sub>Kα</sub>

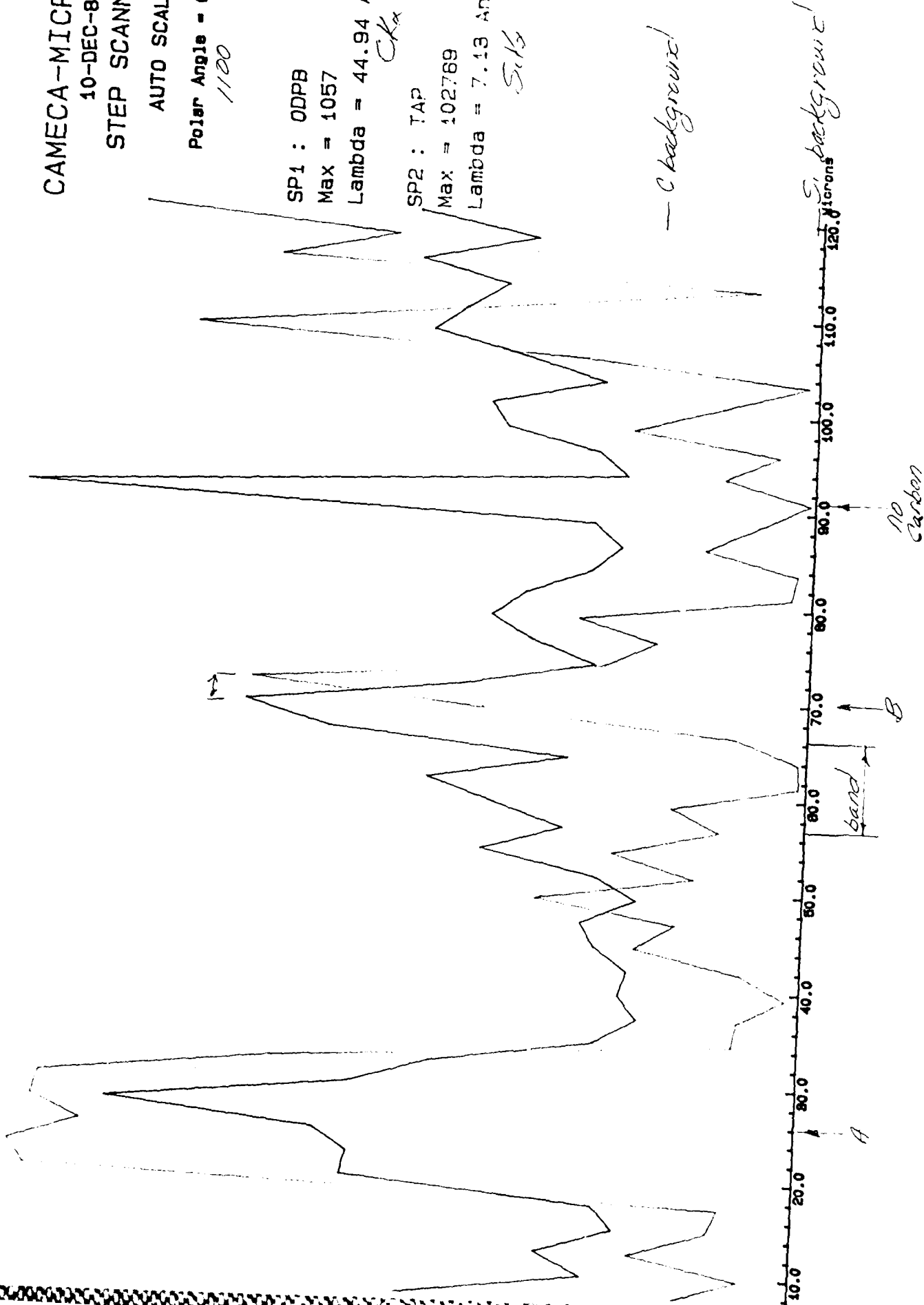


Figure 4. Electron beam microprobe traces for Si and C across heat affected zone, fusion line and weld metal. Path of microprobe trace shown in Figure 1.

CAMECA-MICROBEAM

10-DEC-85

STEP SCANNING

AUTO SCALE

Polar Angle = 0

*Al 3Zr + Si, C*

SP1 : ODPB

Max = 1094

Lambda = 44.94 Angstrom

SP2 : TAP

Max = 99175

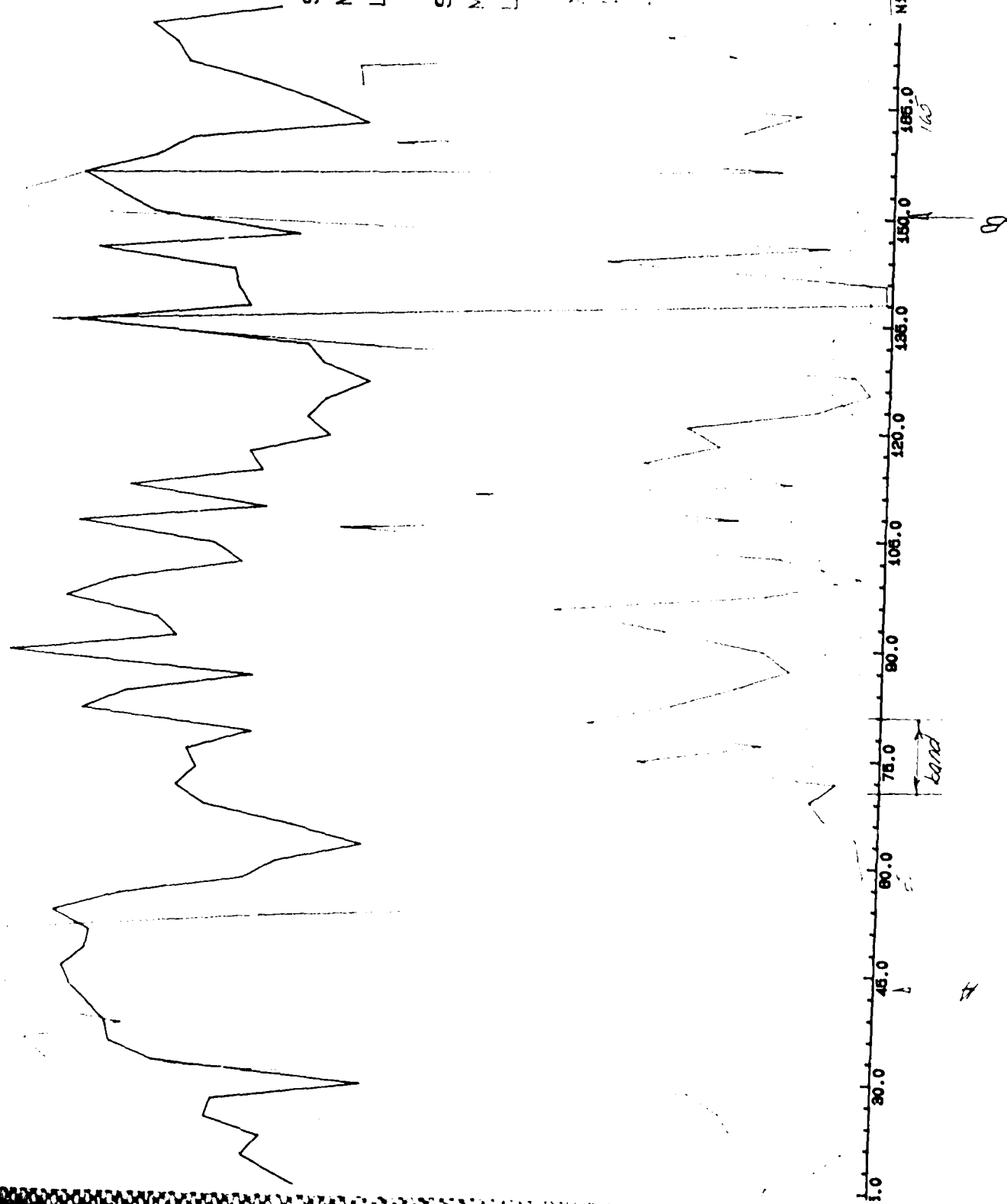
Lambda = 7.13 Angstroms

*Si*

*Al*

Lambda = 0.08 Angstroms

*Zr K*



*S. Lockington*

Figure 5. Electron beam microprobe traces for Si, C, and Zr across heat affected zone, fusion line and weld metal. Path of microprobe trace shown in Figure 2.

CAMECA-MICROBEAM

10-DEC-85

STEP SCANNING

AUTO SCALE

Polar Angle = 0

*A<sub>2</sub>S<sub>2</sub>Ti + S, C*

SP1 : ODPB

Max = 1275

Lambda = 44.94 Angstrom

*C<sub>Kα</sub>*

SP2 : TAP

Max = 104106

Lambda = 7.13 Angstroms

*Si<sub>Kα</sub>*

SP3 : TAP

Max = 104106

Lambda = 7.13 Angstroms

*Ti<sub>Kα</sub>*

*Ti background*

Microns

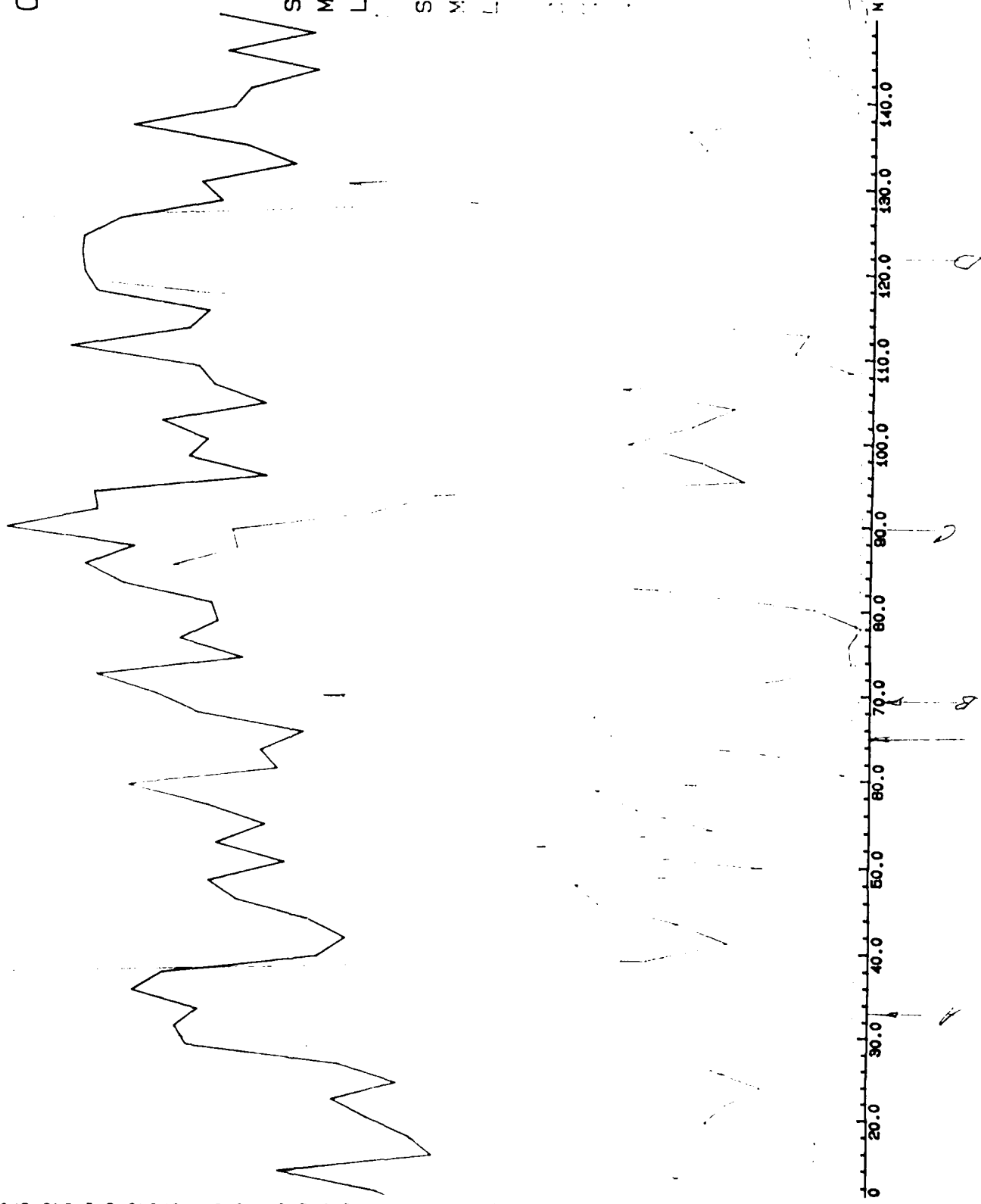


Figure 6. Electron beam microprobe traces for Si, C, and Ti across heat affected zone, fusion line and weld metal. Path of microprobe trace shown in Figure 3.

END

11-87

DTIC